Weierstraß-Institut
für Angewandte Analysis und Stochastik

im Forschungsverbund Berlin e.V.

Preprint ISSN 0946 – 8633

Non-Poissonian statistics in an optical analog of quantum billiard with perfectly square boundaries

I. Babushkin [1]

submitted: 2nd December 2009

[1] Weierstrass Institute for Applied Analysis and Stochastics Mohrenstr. 39, 10117, Berlin, Germany, E-mail: babushkin@wias-berlin.de

No. 1468
Berlin 2009

2000 *Mathematics Subject Classification.* 78A60, 65F15, 15A52.

Key words and phrases. Optical quantum billiards, Semiconductor lasers, Light polarization.

1999 *Physics and Astronomy Classification Scheme.* 05.45.Mt, 42.60.Jf, 42.25.Ja, 42.55.Px.

Edited by
Weierstraß-Institut für Angewandte Analysis und Stochastik (WIAS)
Mohrenstraße 39
10117 Berlin
Germany

Fax: + 49 30 2044975
E-Mail: preprint@wias-berlin.de
World Wide Web: http://www.wias-berlin.de/

Abstract

We study deviation from the Poissonian statistics of the frequency spacing distribution, appearing due to coupling of polarizational and transverse degrees of freedom in a perfectly square vertical cavity surface emitting laser. The deviation can be controlled by strength of the intracavity anisotropy and its alignment to the device boundaries.

1 Introduction

The topics related to 'quantum chaos' constantly attracts a strong attention [1, 2, 3]. In this field behavior of complex quantum- (or wave-) systems is studied, often in relation to integrability of the corresponding classical systems. One of the most known class of systems are quantum billiards. From physical point of view, different types of resonators, ranging from acoustic and microwave resonators to optical cavities and quantum dots (QD) belong to that class. Normally, their behavior is fully determined by the boundaries and in a certain respect reflects the properties of corresponding classical billiards. For simple boundaries (such as square or circle) with fully integrable behavior the frequency spacing (FS) $s_i \sim E_{i+1} - E_i$ of the eigenvalues E_i of the operator $\hat{H}$ determining the system evolution obeys the Poissonian distribution $P(s) = e^{-s}$ (where $P(s)$ is the corresponding probability). In the fully chaotic case the Wigner statistics $P(s) = \frac{\pi}{2}e^{-\pi s^2/4}$ is common [4, 1, 2, 3]. Billiards with their classical counterparts being only partially chaotic demonstrate an intermediate statistics and often referred as 'quasi-integrable' [5, 6].

In more complicated systems as nuclei [3, 7] Wigner distribution does not reflect anymore the complex boundaries but is determined by the complicated nature of the operator $\hat{H}$. In such systems the boundary conditions are often 'trivial' in the sense that they would lead to the integrable behavior in more simple quantum billiard. We will hence refer to the later class of systems as to 'boundary-determined' one whereas the former will be called 'operator-determined' systems.

Many other physical systems beside nuclei posses an operator, complex enough to demonstrate the Wigner or intermediate statistics for simple boundary conditions (or at least to demonstrate a level repulsion), such as atoms and molecules under certain conditions [1, 3], quantum algorithms [8, 9, 10], but also relatively "simple" systems such as acoustic resonators [11] or QD in external field [12, 13, 14].

An example with QD [12, 13, 14] is of especial importance for the present article. An electron in a QD can posses non-Poissonian statistics even for perfectly rectangular boundaries in a presence of external field because the spin of electron is directly connected to its movement direction. In the other words, the internal degrees of freedom (spin) in $\hat{H}$ are coupled to the spatial degrees of freedom defined by boundary conditions. Such quantum billiards belong neither to purely 'boundary-determined' systems nor to purely 'operator-determined', because the boundary conditions are important here. This behavior do not have a classical counterpart because the internal degrees of freedom disappear in the classical limit.

In this article we present an example of such internal-to-spatial degrees of freedom coupling in optics. For electromagnetic waves, microwave resonators and (more recently) microcavity lasers are considered as typical quantum billiards and the internal degree of freedom is represented by the light polarization direction. One of the class of microcavities which becomes recently an attractive object for quantum chaos studies is a vertical cavity surface emitting laser (VCSEL) [15, 16, 17]. An important property of contemporary broad area VCSELs is their high homogeneity in the transverse direction, which allows to consider them as a two-dimensional quantum billiards. In addition, the intracavity anisotropy is rather small allowing simultaneous dynamics of both polarization directions and nontrivial interaction between them.

It was recently shown [18] that in VCSELs an effective anisotropy arises which is different for different transverse propagation directions, thus providing a mechanism for the coupling of polarization and spatial degrees of freedom. In this article we study the deviation from the Poissonian statistics (PS) in the square VCSEL arising due to such coupling. The possibility of such deviation was pointed out in [18]. Here we show that the intracavity birefringence and its alignment to the boundaries play an important role in the above mentioned mechanism, allowing to control this deviation.

2 VCSEL as a quantum billiard

Despite the lasing process has sufficiently nonlinear nature, many properties of the spatio-temporal distribution in broad-area VCSELs can be obtained already in a linear approximation [18]. In this section we consider a linear operator $\hat{H}$ governing the behavior of the optical field in VCSEL close to lasing threshold.

A typical structure of VCSEL is presented in Fig. 1. Although the working area of VCSEL is very homogeneous in the transverse direction, the longitudinal structure of the cavity is rather complicated. The important part is two stacks of $\lambda/4$ layers playing the role of the cavity mirrors (distributed Bragg mirrors (DBRs)) enclosing a thin layer representing a cavity and containing a nonlinear active media.

Despite the complicated longitudinal cavity structure the description of VCSEL can be reduced to exclude the longitudinal degrees of freedom from the consideration [19]. This is possible because VCSEL operates predominantly in a single longitudinal mode. After such reduction and linearization of the resulting equations near lasing threshold [18], the complex longitudinal cavity structure is described by a single

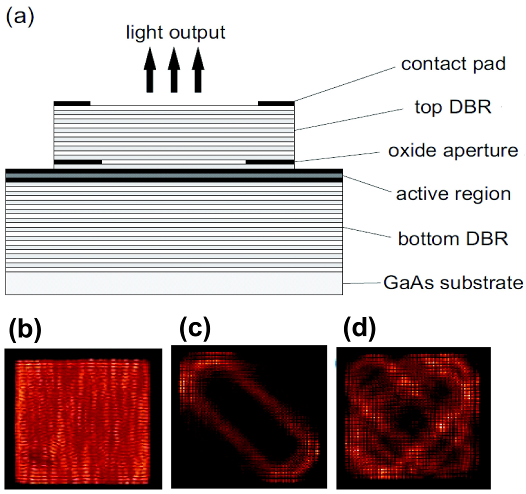

Figure 1: (color online). The longitudinal structure of a typical VCSEL (a), the typical transverse intensity distribution encountered at low temperatures (b)-(d) [23]

linear operator defining evolution of the complex vector field envelope $\mathbf{E}(\mathbf{r}_\perp, t)$ with time:

$$\dot{\mathbf{E}}(\mathbf{r}_\perp, t) = i\hat{H}\mathbf{E}(\mathbf{r}_\perp, t), \tag{1}$$

where dot means the partial time derivative and $\mathbf{r}_\perp = \{x, y\}$ are the transverse coordinates and $\hat{H}$ is a linear operator acting on a set of functions $\mathbf{f}(\mathbf{r}_\perp)$.

It should be noted that the Eq. (1) is valid, strictly speaking, only close to threshold. However, the structure of modes and the dispersion relation defined by this equation is valid also far from threshold [20].

2.1 $\hat{H}$ for transversely infinite device

The operator $\hat{H}$ is most easily described for the infinite VCSEL (i. e. without transverse boundaries). In this case, their eigenfunctions are the tilted waves of the type $\mathbf{E} \sim e^{-i\mathbf{r}_\perp \mathbf{k}_\perp}$ with certain transverse wavevector $\mathbf{k}_\perp = \{k_x, k_y\}$. Therefore, $\hat{H}$ can be written in the transverse Fourier space as a multiplication to a matrix-function $\beta_\infty(\mathbf{k}_\perp)$:

$$\mathcal{F}[\hat{H}\mathbf{E}(\mathbf{r}_\perp, t)] = \beta_\infty(\mathbf{k}_\perp)\mathbf{E}(\mathbf{k}_\perp, t), \tag{2}$$

where $\mathcal{F}[f(\mathbf{r}_\perp)] \sim \int f e^{i\mathbf{r}_\perp \mathbf{k}_\perp} dxdy$ is the transverse Fourier transform. β_∞ is a 2×2-matrix acting on the harmonics of the electric field $\mathbf{E}$ with $\mathbf{k}_\perp$-dependent coefficients. In $\mathbf{k}_\perp$-space Eq. (1) can be written as $\dot{\mathbf{E}}(\mathbf{k}_\perp) = \beta_\infty(\mathbf{k}_\perp)\mathbf{E}(\mathbf{k}_\perp)$.

Close to lasing threshold, losses and gain in laser compensate each other, therefore the operator $\hat{H}$ is rather close to Hermitian one. For simplicity, in the following we *neglect the non-hermitian part of the operator.* In this approximation (and assuming the laser infinite in transverse directions) the matrix β_∞ can be written as

$$\beta_\infty(\mathbf{k}_\perp) = ak_\perp^2 + \Gamma + bs(\mathbf{k}_\perp), \tag{3}$$

where a and b are the parameters defined by the device structure, $k_\perp = |\mathbf{k}_\perp|$ is the modulus of transverse wavevector (and hence the first term in Eq. (3) represents the 'trivial' part of our billiard problem, i.e. the kinetic energy of free-moving 'particle'). The second term is the intracavity phase anisotropy, which in the Cartesian basis formed by principal anisotropy axis can be written as $\Gamma = \mathrm{diag}(\gamma_p, -\gamma_p)$, where $\mathrm{diag}(\cdot,\cdot)$ is a 2×2 diagonal matrix with corresponding elements on the diagonal, γ_p is strength of the anisotropy. The amplitude anisotropy is neglected in the present consideration.

The matrix $s(\mathbf{k}_\perp)$ represents the DBR reflection phases. In the infinite device, the reflection from DBR can be represented by a $\mathbf{k}_\perp$-depended matrix $R(\mathbf{k}_\perp)$, so that the reflected field $\mathbf{E}_r(\mathbf{k}_\perp)$ is connected to the incident field $\mathbf{E}_i(\mathbf{k}_\perp)$ as $\mathbf{E}_r = R\mathbf{E}_i$. The ($\mathbf{k}_\perp$-dependent) eigenvectors of R are named s- and p- waves and have polarization parallel and perpendicular to $\mathbf{k}_\perp$, correspondingly (i.e. they are radially and azimuthal polarized). In the polarization basis, which axes coincide with s- and p- waves R has a form $R = \mathrm{diag}(R_s, R_p)$ with $R_s = |R_s|e^{is_s}$, $R_p = |R_p|e^{is_p}$ being the reflections for s- and p- waves with corresponding phases s_s and s_p [21, 22]. In the following we assume that the both reflectors are equivalent. Under these conditions, $s = \mathrm{diag}(s_s, s_p)$. Because s is $\mathbf{k}_\perp$ dependent matrix and in general $s_s \neq s_p$, the last term in Eq. (3) introduces a $\mathbf{k}_\perp$-dependent anisotropy.

2.2 Reduction to a square aperture

The theory above was developed for an infinite device. Now we introduce square boundaries determined physically by the oxidation aperture which leads to a guiding of the cavity modes in the transverse direction. The modes of a square waveguide (neglecting the rest of the cavity) can be under certain simplifications written as $\mathbf{E}_{nm}^{(x)} = f_n(\pi x/a)f_m(\pi y/a)\mathbf{n}_x$, $\mathbf{E}_{nm}^{(y)} = f_n(\pi x/a)f_m(\pi y/a)\mathbf{n}_y$, where a is the waveguide size, $\mathbf{x}$, $\mathbf{y}$ are unit vectors in corresponding directions, $f_n(z) = \cos(nz)$ if n is odd and $\sin(nz)$ if n is even.

In the terms of the $\mathbf{k}_\perp$ they are nothing but a four-spot configurations in $\mathbf{k}_\perp$-space (see Fig. 2):

$$\mathbf{k}_1 = (k_x, k_y),\ \mathbf{k}_2 = (k_x, -k_y), \tag{4}$$
$$\mathbf{k}_3 = (-k_x, k_y),\ \mathbf{k}_4 = (-k_x, -k_y). \tag{5}$$

For the case of the whole cavity (taking account also the DBRs) the situation becomes more complicated. The modes of the waveguide are polarizationally degenerate. Therefore, any combination of the two modes with fixed k_x, k_y in Eq. (4) (but different polarizations) is also a waveguide eigenmode. However, no of these modes are also the modes of DBRs, because the directions of DBR mode polarization are

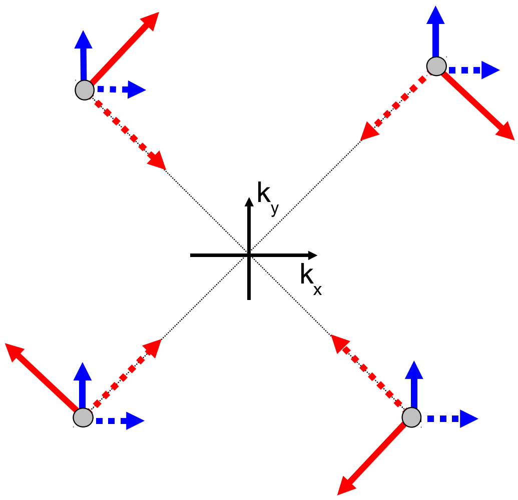

Figure 2: (color online). The polarizational mode structure of DBR and waveguide modes in a square VCSEL in $\mathbf{k}_\perp$-plane. The mode structure of the waveguide is given by four spot configuration (see Eq. (4)) with equal polarization in every spot (short blue arrows). In contrast, the polarization eigen-directions of the DBR modes (long red arrows) are either parallel or perpendicular to $\mathbf{k}_\perp$ in every spot. Possible orthogonally-polarized configurations arte marked by either solid or dashed line styles.

different for every $\mathbf{k}_\perp$-spot (Fig. 2, red long lines). Therefore, no combination of waveguide mode with wavenumber k_x, k_y is an eigenfunction of the full problem Eq. (1) with square boundary conditions.

The eigenfunctions of Eq. (1) exist, but they are thus the combinations of the waveguide modes with different wavevectors $\mathbf{k}_\perp$. Physically that means, that reflection from DBR rescatters the eigenmodes of the waveguide into another waveguide modes (with different $\mathbf{k}_\perp$). This rescattering creates in essence the connection between the transverse and polarizational degrees of freedom because it is purely 'vectorial' effect and disappear if we do not take into account polarization [18].

We can construct the operator acting on the modes of the waveguide β_c using β_∞ as a starting point. We then provide extension of β to the four-spot configuration of Eq. (4), Eq. (5), which gives us the operator $\beta_k = \operatorname{diag}\{\beta(\mathbf{k}_1), \beta(\mathbf{k}_2), \beta(\mathbf{k}_3), \beta(\mathbf{k}_4)\}$ ($\operatorname{diag}(\ldots)$ is 8×8 block-diagonal matrix with corresponding 2×2 matrices on the diagonal). Then we transform the matrix to the basis of $\cos(k_x x), \cos(k_y y), \sin(k_x x), \sin(k_y y)$ functions (from a $\exp(ik_x x + ik_y y)$ one, which a describe single spot in $\mathbf{k}_\perp$ space):

$$\beta_c = S\beta_k S^{-1}, \tag{6}$$

where matrix S is

$$S = \frac{1}{4}\begin{pmatrix} \mathbb{1} & \mathbb{1} & \mathbb{1} & \mathbb{1} \\ -i\cdot\mathbb{1} & -i\cdot\mathbb{1} & i\cdot\mathbb{1} & i\cdot\mathbb{1} \\ -i\cdot\mathbb{1} & i\cdot\mathbb{1} & -i\cdot\mathbb{1} & i\cdot\mathbb{1} \\ -\mathbb{1} & \mathbb{1} & \mathbb{1} & -\mathbb{1} \end{pmatrix}, \tag{7}$$

where $\mathbb{1} = \left(\begin{smallmatrix} 1 & 0 \\ 0 & 1 \end{smallmatrix}\right)$ is a 2×2 unit matrix.

The matrix β_c is defined on a space more general than the one formed by the simple waveguide modes, because it contains arbitrary combinations of $\sin, \cos$ functions. The "suspicious" modes in β_c are rescattered into the true waveguide modes with different $\mathbf{k}_\perp$. We then obtain the resulting operator β_s.

$$\beta_s^{ijklmn} = \sum_{i'j'k'l'm'n'} T^{ijklmn}_{i'j'k'l'm'n'} \beta_c^{i'j'k'l'm'n'}, \tag{8}$$

where T is an operator defined below, i, j, i', j' are polarization indices taking values x and y, k, l, k', l' are the indices numbering the x-indices of transverse modes (i. e., for example, $\sin(\pi kx/a)$ or $\cos(\pi lx/a)$) and m, n, m', n' are the corresponding y-indices. The resulting matrix β_s^{ijklmn} acts on the field as

$$E^{(i)}_{km} = \sum_{j,l,n} \beta_s^{ijklmn} E^{(j)}_{ln}, \tag{9}$$

The elements of operator $T^{ijklmn}_{i'j'k'l'm'n'}$ are given by the expression (up to normalizing constant):

$$T^{ijklmn}_{i'j'k'l'm'n'} = \int_{-a/2}^{a/2} f_k^{(i)} f_m^{(i)} f_{k'}^{(i')} f_{m'}^{(i')} f_l^{(j)} f_n^{(j)} f_{l'}^{(j')} f_{n'}^{(j')} dxdy, \tag{10}$$

where by $f_m^{(i)}$ the vectorial extensions of functions f_m are denoted: $f_m^{(x)} = \{f_m, 0\}$ and $f_m^{(y)} = \{0, f_m\}$. Not all the elements of T off the diagonal (which represent rescattered modes) are zeros. The integrals in Eq. (10) can be elementary calculated analytically for every particular combination of indexes. In general, non-diagonal elements are decaying as $\sim \frac{1}{k-l}\frac{1}{m-n}$ off the main diagonal ($k = l$, $m = n$).

The matrix β_s^{ijklmn} represents the operator $\hat{H}$ in basis of waveguide modes. For the purposes of comparison let us define now the matrix β_p, where the coupling of polarization and transverse degrees of freedom is neglected. In such matrix, we neglect the modes which are rescattered to the other wavevectors due to unmatching of the polarizations of DBRs and the waveguide (as shown in Fig. 2). It can be written in terms of components of the full matrix β_s:

$$\beta_p^{ijklmn} = \delta_{kl}\delta_{nm}\beta_s^{ijklmn}, \tag{11}$$

where δ_{nm} is the Kronecker δ-symbol.

2.3 Numerical procedure

The set of indices β_s^{ijklmn} represent the operator $\hat{H}$ in basis of waveguide modes. For numerical computation of the eigenvalues of such operator one have to transform it into a square matrix. It can be done by introducing the indices $I = i + 2k + 2(N_{\max} - N_{\min} + 1)m$, $J = j + 2l + 2(N_{\max} - N_{\min} + 1)n$ where $N_{\max}$ and $N_{\min}$ are the maximal and minimal possible indexes in f_n (defined by cutoff). In numerical simulation, a cut-off of high as well as low order modes were made. Physically the high order modes are cut-off because they are not guided by the effective waveguide formed by the oxidation layer anymore. On the other hand, we are trying to model physical situation where predominantly high enough transverse modes are exited. Therefore we cut-off also the modes of lowest order to reduce the matrix size. For the simulations the values $N = 40$, $N_{min} = 20$ were taken. This reasonably represents the mode selection in real devices [15, 18]. The matrix $\beta_s^{I,J}$ is therefore a matrix of the size $\sim 882 \times 882$ with corresponding number of eigenvalues.

3 The FS distribution

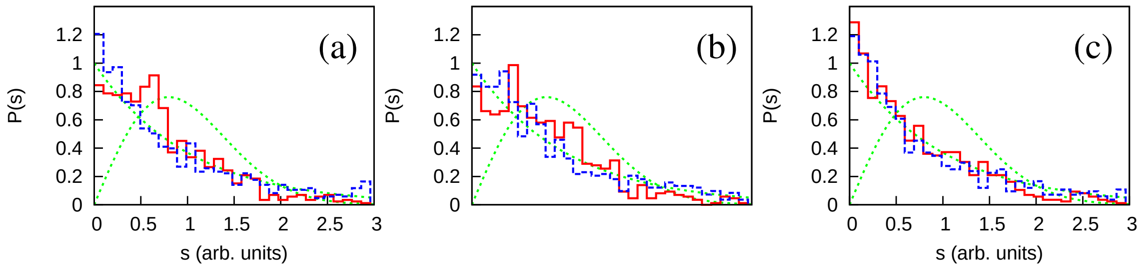

Figure 3: (color online). Statistics of the eigenvalues of β_s (red solid curves) and β_p (blue dot-dashed curves) for different intracavity anisotropies Γ (in particular for different strengths γ_p and angles α of the main anisotropy axes in respect to x-axis). (a) — $\gamma_p = 30$ ns^{-1}, $\alpha = \pi/15$; (b)—$\gamma_p = 60$ ns^{-1}, $\alpha = \pi/15$; (c)—$\gamma_p = 30$ ns^{-1}, $\alpha = 0$; For comparison, the Poisson and Wigner statistics are plotted by green dotted lines.

The statistics $P(s)$ of FS $s_i \sim E_{i+1} - E_i$ of the eigenvalues E_i of the matrices β_s and β_p is presented in Fig. 3 for typical VCSEL parameters [18, 23].

For the Fig. 3(a) the birefringence γ_p is 30 ns^{-1} and the anisotropy axes are rotated to the angle $\pi/15$ to the direction of x-axis. One can see that the the FS distribution of the matrix β_s (Fig. 3(a), red solid curve) is in between the Poissonian one and the Wigner one (Fig. 3(a), green dotted curves). At it was mentioned in the previous section, the matrix β_s is the the representation of the operator $\hat{H}$ in the basis of the square waveguide modes and includes the interaction of transverse and polarization degrees of freedom. In contrast, for the matrix β_p (with excluded transverse-polarization interaction) the FS distribution is very close to the Poissonian one (Fig. 3(a), green dashed curve).

From the previous it is follows that the polarization-spatial coupling is critical for the deviation from the PS. The intracavity anisotropy (which is $k_\perp$-independent anisotropy), including its value and the tilt of the main axis in respect to the VCSEL boundaries is an another critical parameter determining the spectral properties of

β_s. As the strength of the anisotropy γ_p increases (see Fig. 3(b)), the deviation from PS decreases (although does not disappear at all). This behavior can be explained in the following way: for large γ_p, the intracavity anisotropy "overcomes" the Bragg-induced anisotropy in the sense, that the later plays less noticeable role in determination of polarization of the eigenmodes. In the other words, with $\gamma_p \to \infty$ the polarization degree of freedom "disappears" from the system.

In the other limit $\gamma_p \to 0$ the deviation from PS also becomes less noticeable. Moreover, for $\gamma_p \neq 0$, if the angle α of the intracavity anisotropy axis (to the x-axis, which is directed along one of the boundaries) is zero, the statistics becomes again Poissonian (see Fig. 3(c)). This shows that the relation between the anisotropy axes and the boundaries is another condition necessary for the deviation from PS, beside the polarization-transverse coupling. In real devices, although the anisotropy is, as a rule, aligned approximately to the boundaries due to the fabrication process, some small misalignment as large as several degrees is present sometimes [23].

4 Discussion and Conclusions

As a conclusion, we have shown that the coupling of transverse and polarizational degrees of freedom in slightly-anisotropic VCSEL, which appears due to distributed Bragg reflectors (DBRs), can lead to deviation of the spacing distribution from the Poissonian one even in perfectly square geometry.

The quantum billiard problem defined by Eq. (1) can be considered as a perturbation of a "free movement" described by $\hat{H} \sim \Delta$ (see Eq. (3)) with the term $\hat{s} + \Gamma$ as a perturbation (here $\hat{s}$ is the operator in the coordinate space corresponding to $s(\mathbf{k}_\perp)$ in Eq. (3)). The part $\hat{s}$ is responsible for the polarization-transverse coupling. In the presence of the misalignment of the intracavity anisotropy to the boundaries the above mentioned rescattering becomes more "chaotic" and the spacing distribution deviates from the Poissonian one.

The above mentioned perturbation is the essentially non-classical one because it relies on the internal degrees of freedom of photons having no classical counterpart. The mechanism presented here is also different from the one presented in [24], which appears in periodically modulated optical waveguides (an optical analog of a periodically-forced system). In particular, in contrast to [24], the deviation from PS in VCSEL disappears in a circular geometry [17] because the term $\hat{s}$ is isotropic in this case.

In the present article, we fully disregarded the losses in the system. Although this can be an acceptable approximation close to threshold (where losses are just compensated by a gain), it is known that the presence of losses can influence the statistics. This will be an interesting direction for the further study of the present system.

References

[1] H.-J. Stöckmann, Quantum Chaos: An Introduction, Cambridge University Press, New York, USA, 1999.

[2] P. Cvitanović et al., Chaos: Classical and quantum, e-book: http://www.chaosbook.org/ (2009).

[3] T. Guhr, A. Müller-Groeling and H. A. Weidenmüller, Random-matrix theories in quantum physics: common concepts, Phys. Rep. 299 (4-6) (1998) 189.

[4] S. W. McDonald, A. N. Kaufman, Phys. Rev. Lett. 42 (18) (1979) 1189.

[5] E. Bogomolny, C. Schmit, Phys. Rev. Lett. 92 (24) (2004) 244102.

[6] E. Bogomolny, et al., Phys. Rev. Lett. 97 (25) (2006) 254102.

[7] H. A. W. T. Papenbrock, Random matrices and chaos in nuclear spectra, Rev. Mod. Phys. 79 (2007) 997.

[8] D. Braun, Phys. Rev. A 65 (4) (2002) 042317.

[9] I. Kim, G. Mahler, Phys. Lett. A 263 (4-6) (1999) 268.

[10] B. Georgeot, D. L. Shepelyansky, Phys. Rev. E 62 (5) (2000) 6366.

[11] K. Schaadt, A. Kudrolli, Phys. Rev. E 60 (4) (1999) R3479.

[12] M. A. M. de Aguiar, Phys. Rev. E 53 (5) (1996) 4555.

[13] K.-F. Berggren, T. Ouchterlony, Found. Phys. 31 (2001) 233.

[14] M. Novaes, M. A. M. de Aguiar, Phys. Rev. E 70 (4) (2004) 045201.

[15] K. F. Huang, Y. F. Chen, H. C. Lai, Y. P. Lan, Phys. Rev. Lett. 89 (22) (2002) 224102.

[16] Y. F. Chen, K. F. Huang, H. C. Lai, and Y. P. Lan, Phys. Rev. E 98 (2) (2003) 026210.

[17] T. Gensty et al., Phys. Rev. Lett. 94 (23) (2005) 233901.

[18] I. V. Babushkin et al., Phys. Rev. Lett. 100 (21) (2008) 213901.

[19] N. A. Loiko, I. V. Babushkin, Journ. Opt. B: Quant. Semiclass. Opt. 3 (2) (2001) S234.

[20] M. Schulz-Ruhtenberg et al., Appl. Phys. B 81 (7) (2005) 945.

[21] D. I. Babic, N. Dagli, J. E. Bowers, IEEE Journ. Quant. Electron. 29 (6) (1993) 1950.

[22] M. Born, E. Wolf, Principles of Optics: Electromagnetic Theory of Propagation, Interference and Diffraction of Light, 6th Edition, Cambridge University Press, 1997.

[23] M. A. Schulz-Ruhtenberg, Experimental analysis of spatial states in broad-area vertical-cavity surface-emitting lasers, Ph.D. thesis, Westfälische Wilhelms-Universität Müster (2008).
URL http://nbn-resolving.de/urn:nbn:de:hbz:6-14549409755

[24] O. Agam, S. Fishman, R. E. Prange, Phys. Rev. A 45 (9) (1992) 6773.